2014 IEEE International Conference on Acoustic, Speech and Signal Processing (ICASSP)

A Nonlinear Ultrasound Propagation Simulator using the Slowly Varying Envelope Approximation

Clément Marti, François Varray, Christian Cachard
Université de Lyon, CREATIS
CNRS UMR5220, Inserm U1044, INSA-Lyon, Université Lyon 1, France
Email: francois.varray@creatis.insa-lyon.fr

***Abstract*—Traditional ultrasound imaging takes into account linear propagation only. However, new methods seek to exploit the nonlinear properties of tissues, which create a specific contrast source. Optimizing these methods require simulating the pressure field in the media at a reasonable computational cost. This paper details how using the Slowly Varying Envelope Approximation (SVEA), a method coming from nonlinear optics, enables to compute several harmonics generated by nonlinearity. This simulator is suited to media with a nonlinearity coefficient varying in all 3 spatial dimensions. SVEA one-way field predictions are compared with those of three other simulators up to the fifth harmonic, showing a good agreement up to 1.1 dB depending on the simulator. This method runs on desktop computers in less than 8 minutes for a 128x128x512x400 discretization grid.**

I. Introduction

Most clinical applications of ultrasound imaging are based on linear propagation: a pulse with a given frequency is sent out by the probe, propagates in the medium and after scattering a part comes back to the probe at the same frequency. However, biological media exhibit a nonlinear behaviour, which can be enhanced by the use of ultrasound contrast agents: the returning ultrasound pulse contains more frequencies than the one sent out and numerous harmonics are present. Nonlinear ultrasound imaging seeks to exploit these additional frequencies, as they can bring information about the nature of tissues, or enhance the resolution. The development of these techniques drives the need for simulation tools able to help to optimize ultrasound setups, for instance by studying many probe designs in a short time. The main approaches in the ultrasound community are based on the finite difference method [1] and the angular spectrum method (ASM) [2] [3]. The first one computes derivatives at each point of a 3D+t grid. The second uses the Fourier Transform to represent the problem. This paper presents an extension of the ASM using the Slowly Varying Envelope Approximation (SVEA), a method coming from nonlinear optics, and details its implementation. The following part describes the mathematical background of ASM and SVEA and its implementation. Then, the results from SVEA are compared to those of other simulators. Finally, a discussion closes the paper.

II. Mathematical background

A. Angular Spectrum Method

The equation describing the nonlinear propagation of an ultrasound wave of pressure p is the lossless Westervelt equation

$$\Delta p - \frac{1}{c_0^2}\frac{\partial^2 p}{\partial t^2} = -\frac{\beta}{\rho_0 c_0^4}\frac{\partial^2 p^2}{\partial t^2} \tag{1}$$

with β being the nonlinearity coefficient, ρ_0 the medium density at rest, c_0 the sound velocity and $\Delta = \frac{\partial^2}{\partial x^2} + \frac{\partial^2}{\partial y^2} + \frac{\partial^2}{\partial z^2}$ the Laplacian. The ASM relies on the 2D+t Fourier Transform (FT) F_{xyt} of the field along spatial dimensions x and y and the time dimension t. The FT separability gives

$$P = F_{xyt}(p) = F_{xy}(F_t(p)) \tag{2}$$

with

$$\begin{cases} F_{xy}(p) &= \displaystyle\int_{-\infty}^{+\infty} e^{-i(k_x x + k_y y)} dx dy \\ F_t(p) &= \displaystyle\int_{-\infty}^{+\infty} e^{i\omega t} dt \end{cases} \tag{3}$$

These definitions have the following useful properties

$$\begin{cases} F_{xyt}(\frac{\partial^n p}{\partial t^n}) &= (i\omega)^n F_{xyt}(p) \\ F_{xyt}(\frac{\partial^n p}{\partial u^n}) &= (-ik_u)^n F_{xyt}(p) \end{cases} \tag{4}$$

with u being x or y.

Applying the FT to (1) and using the properties in (4) leads to

$$-(k_x^2 + k_y^2)P + \frac{\partial^2 P}{\partial z^2} + \frac{\omega^2}{c_0^2}P = -\frac{1}{\rho_0 c_0^4} F_{xyt}\left(\beta \frac{\partial^2 p^2}{\partial t^2}\right) \tag{5}$$

Because β does not change over time and only depends on spatial dimensions,

$$\beta \frac{\partial^2 p^2}{\partial t^2} = \frac{\partial^2 \beta p^2}{\partial t^2} \tag{6}$$

So using (6) and (4) on the right-hand side of (5) it can be rewritten as

$$\frac{\partial^2 P}{\partial z^2} + k_z^2 P = \frac{\omega^2}{\rho_0 c_0^4} F_{xyt}(\beta p^2) \tag{7}$$

where $k_z^2 = {\omega^2}/{c_0^2} - (kx^2 + k_y^2)$ is the squared projection of the wave vector along the axis z for a wave of pulsation ω and wave vector projection (k_x, k_y) in the (x, y) plane. A more detailed derivation of this equation can be found in [4].

When $\beta = 0$, the solution of (7) for forward-propagation only is

$$P = P_{z_0} e^{-ik_z z} \tag{8}$$

with $P_{z_0} = F_{xyt}(p_{z_0})$ the Fourier Transform of the initial transmitted pressure wave.

B. Slowly Varying Envelope Approximation

Let H so that

$$H = P e^{ik_z z} \tag{9}$$

H is the complex amplitude, also called envelope, of a wave of vector (k_x, k_y, k_z) and pulsation ω. If there is no nonlinearity in the medium and only forward propagation is taken into account, this envelope remains constant along z.

Using definition (9) yields:

$$\frac{\partial^2 P}{\partial z^2} = \frac{\partial^2 H}{\partial z^2} e^{-ik_z z} - 2ik_z \frac{\partial H}{\partial z} e^{-ik_z z} - k_z^2 H e^{-ik_z z} \tag{10}$$

So using (10) and (9), $k_z^2 H e^{-ik_z z}$ simplifies in (7) and it becomes

$$\frac{\partial^2 H}{\partial z^2} e^{-ik_z z} - 2ik_z \frac{\partial H}{\partial z} e^{-ik_z z} = \frac{\omega^2}{\rho_0 c_0^4} F_{xyt}(\beta p^2) \tag{11}$$

Under the assumption that the characteristic length of variation of H is high compared to $1/k_z$,

$$\left| \frac{\partial^2 H}{\partial z^2} \right| << \left| k_z \frac{\partial H}{\partial z} \right| \tag{12}$$

This is the Slowly Varying Envelope Approximation (SVEA). It is widely used in nonlinear optics [5] [6] and has the property of taking into account only forward-propagating new harmonics. Since k_z is in the right hand side of the inequality (12), the approximation is better for waves propagating in the direction of the axis z. With this assumption the higher order derivatives can be neglected and (11) becomes:

$$\frac{\partial H}{\partial z} = \frac{i\omega^2}{2k_z \rho_0 c_0^4} F_{xyt}(\beta p^2) e^{ik_z z} \tag{13}$$

the solution of which is:

$$H(z) = H_{z_0} + \int_{z_0}^{z} \frac{i\omega^2}{2k_z \rho_0 c_0^4} F_{xyt}(\beta p^2) e^{ik_z u} du \tag{14}$$

Which can be used to get the pressure field at depth z:

$$p(z) = F_{xyt}^{-1}(H(z) e^{-ik_z z}) \tag{15}$$

C. Discretization and Attenuation

Equation (14) lends itself to numerical integration through an explicit Euler method. For a step size dz along z it consists in iterating

$$H(z + dz) = H(z) + \frac{i\omega^2}{2k_z \rho_0 c_0^4} F_{xyt}(\beta p^2) e^{ik_z z} dz \tag{16}$$

Up to this development, attenuation by the medium was not taken into account since it is not modeled by (1), only diffraction and nonlinearity were. Attenuation in biological media depends on the frequency $f = \omega/2\pi$ and is described for monochromatic waves propagating along an axis u by the empirical law [7]:

$$\frac{\partial p}{\partial u} = -\alpha_0 f^\gamma p \tag{17}$$

which translates for H for a step dz, assuming waves are paraxial and taking only attenuation into account, as

$$H(z + dz) = e^{-\alpha_0 f^\gamma dz} H(z) \tag{18}$$

A development to accurately extend this to non-paraxial waves can be found in [8]. So at first order, with attenuation taken into account (16) becomes

$$H(z + dz) = e^{-\alpha_0 f^\gamma dz} H(z) + \frac{i\omega^2}{2k_z \rho_0 c_0^4} F_{xyt}(\beta p^2) e^{ik_z z} dz \tag{19}$$

D. Computer implementation

The above described discretization has been implemented on CPU using the C++ language and the FTTW library [9] to perform the FT. p_{z_0} depends on the probe parameters detailed in Table I. The implemented algorithm is summed up in algorithm 1.

Algorithm 1 SVEA implementation

$H \leftarrow F_{xyt}(p_{z_0})$
$N \leftarrow \dfrac{i\omega^2}{2k_z \rho_0 c_0^4} dz$
$p \leftarrow p_{z_0}$
$A \leftarrow e^{-\alpha_0 f^\gamma dz}$
$z \leftarrow 0$
while $z < z_{max}$ **do**
  $z \leftarrow z + dz$
  $H \leftarrow AH + N F_{xyt}(\beta p^2) e^{ik_z z}$
  $p \leftarrow F_{xyt}^{-1}(H e^{-ik_z z})$
  Save p
end while

III. Comparison with other simulators

A. Simulation tools

For comparison purposes, three other simulators were used: the well known FieldII simulator [10], which can not take into account nonlinearity and is consequently used as a baseline for the field at the fundamental frequency, the INCS simulator by J. Huijssen [11] and the finite difference KZK simulator by M. Voormolen [1], [12]. The latter uses the Kuznetsov-Zabolotskaya-Khokhlov equation [13], [14] instead of the Westervelt equation. A transmitted pulse at fundamental frequency $f_0 = 1$ MHz and maximum pressure on the transducer $p_0 = 1$ MPa was chosen. The high pressure favors the generation of harmonics. Fig. 1 displays the SVEA and KZK field predictions for several harmonics in the plane normal to the probe and their relative difference. The relative difference d_i between the ith harmonics of the SVEA and of the KZK is estimated with

$$d_i = 2 \frac{|p_i^{KZK} - p_i^{SVEA}|}{p_i^{KZK} + p_i^{SVEA}} \tag{20}$$

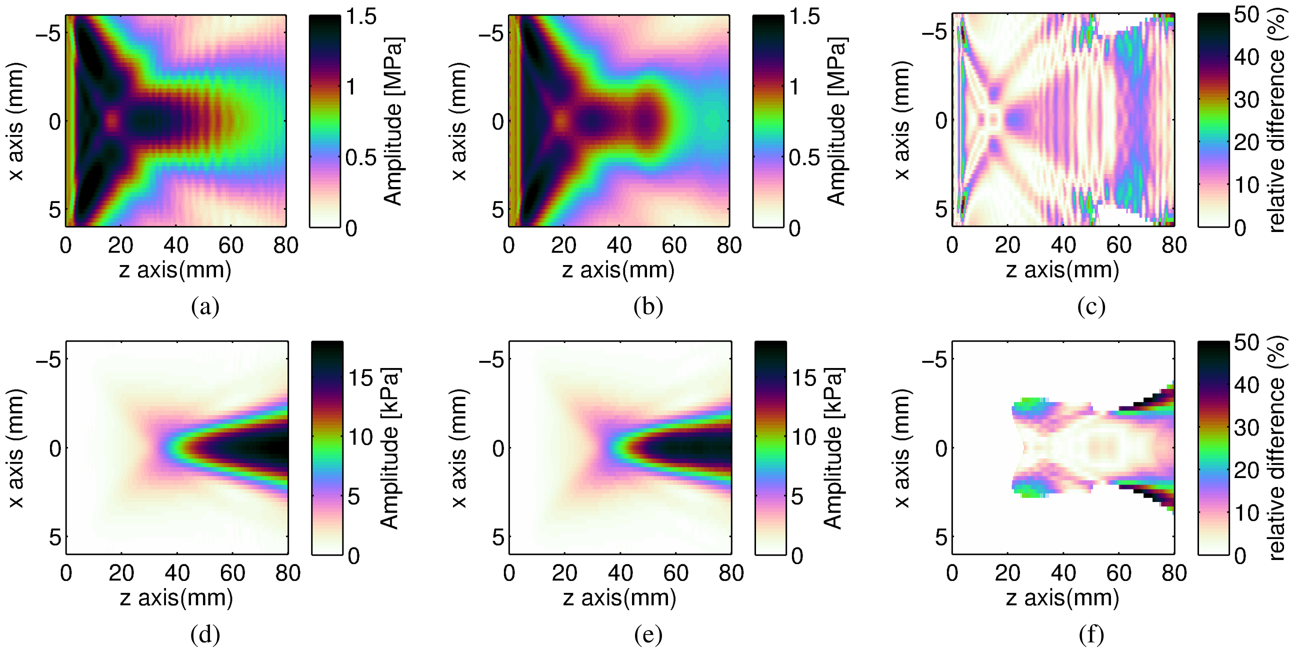

Fig. 1. SVEA (a,d) and KZK (b,e) predictions and relative difference (c,f) between the two simulators. First line corresponds to the first harmonic, second line to the fourth.

d_i is only displayed for pixels where p_i^{SVEA} is over 10% of its maximum value, because the field has a low intensity outside the main beam and d_i is then very sensitive to small absolute differences between maximum pressures. Fig. 2 shows the evolution of p_i^{SVEA}, p_i^{INCS}, p_i^{KZK} along the z axis. p^{FII}, the maximal pressure over time at the fundamental frequency as computed by FieldII is also shown. Probe and medium parameters are given in Table I.

B. Evaluation

1) Axial profile: As Fig. 2 shows, the SVEA stays within 2.0 dB compared to the INCS for the fundamental frequency. For the others harmonics, the predicted field is much higher for small z and the gap increases with frequency. However, as z increases and the field generated by nonlinear effect grows stronger the discrepancy decreases: at $z = 6.6$ mm, the second harmonic field has reached 10% of its maximum intensity and the INCS and SVEA predictions are separated by 5.1 dB. For the 5th harmonic, 10% of maximum intensity is reached at $z = 35$ mm, where the difference between INCS and SVEA is 4.5 dB. For all harmonics, the difference is lower than 2.0 dB at $z = 80$ mm.

The SVEA has a better fit with the KZK simulator than with the INCS, especially for small z: at $z = 6.6$ mm, the second harmonics are separated by 1.6 dB, at $z = 35$ mm, the 5th harmonics are separated by 3.7 dB. At $z = 80$ mm, the difference is lower than 1.8 dB for all harmonics.

Compared to FieldII, the SVEA stays within 1.1 dB for $z > 3$ mm. Before this point, the FieldII prediction exhibits a sudden decrease in intensity not present with other simulators which is likely a near-field artifact.

2) Relative difference: As seen in Fig. 1, the relative difference between SVEA and KZK is higher on the edges of the main beam where the intensity drops near 10% of the maximum. In the main beam, d_i is mostly under 30%. This is coherent with the previous analysis of the axial profile, since the discrepancy was higher where the pressure was lower.

C. Pratical aspects

The extraction of the pressure field in the different frequency bands was performed using MATLAB (The MathWorks, Natick, United States) by zero-phase filtering the field with passband Butterworth filters of order 10 and of double-sided bandwidth 1 MHz, at central frequencies f_0 to $5f_0$ by increments of f_0, and then taking the maximum over time for each pixel.

The SVEA simulation was performed on a standard laptop (Intel core i7-3612QM @ 2.1GHz, 8GB of memory) with a C++ program. With the high sampling mentioned in Table I, the computation took less than 8 minutes.

IV. Discussion and Conclusion

The SVEA is an approximation and thus has a limited domain of validity. However, one can keep track of (12) to know if it is not justified, which is the case in the presented simulation. The comparison between SVEA and other simulators shows that in the regions where the intensity of harmonics is strong the SVEA predictions are consistent with the others. These regions are those of interest for clinical applications since they present the strongest echoes: other regions are hardly visible in harmonic imaging, since probes have a limited sensitivity. The SVEA is also a flexible method, since it allows for variations of the β parameter in all spatial

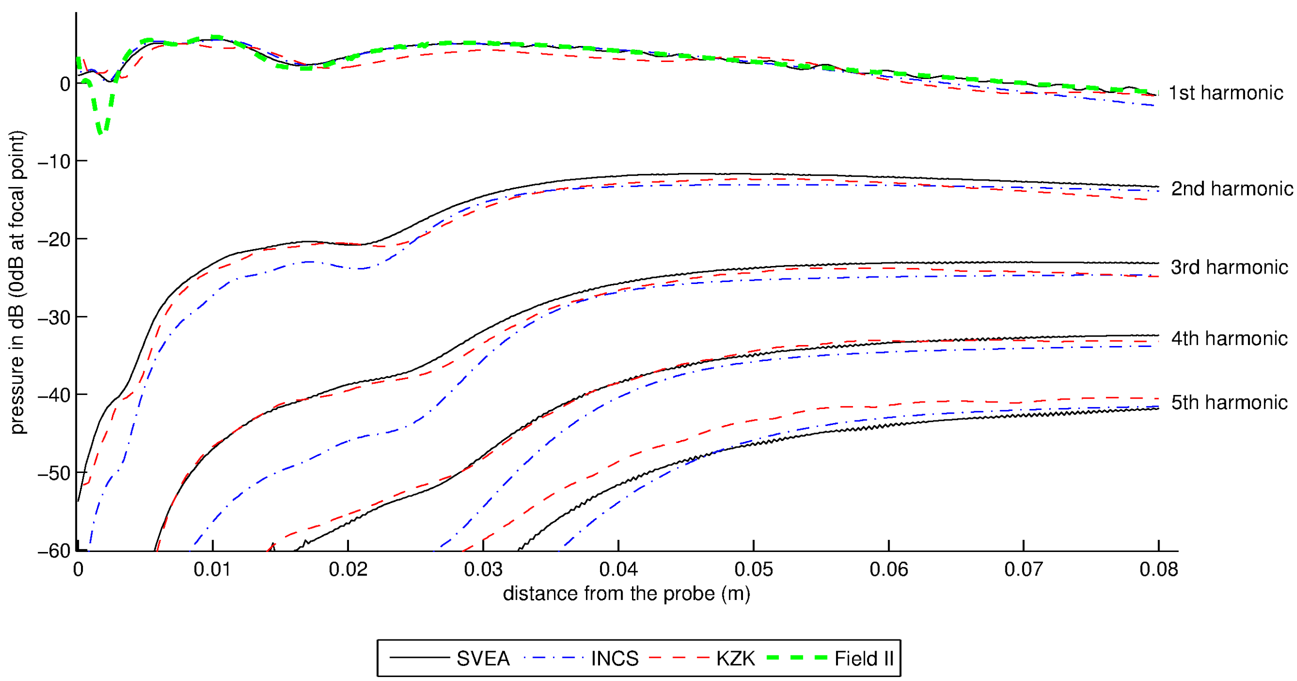

Fig. 2. Axial pressure profiles for harmonics 1 to 5 with the SVEA, INCS, KZK and Field II simulators

TABLE I
SIMULATION PARAMETERS

Parameter	Value
Pitch	245 µm
Kerf	30 µm
Element height	6 mm
Number of elements	64
(x, y, z) coordinates of focus	(0,0,70 mm)
elevation	23 mm
apodization	none
f_0	1 MHz
p_0	1 MPa
speed of sound in medium	1540 m.s^{-1}
medium density	1000 kg.m^{-3}
α_0	0.025 Np.m^{-1}.MHz$^{-\gamma}$
γ	2
number of discrete points in x, y, z and t	128, 128, 400, 1024

dimensions, and can also deal with variations of α_0 and γ in the z direction without changing the formalism: the only change in Algorithm 1 is to recompute the attenuation matrix A at each step. Thus, investigation of realistic media is facilitated. Allowing these parameters to vary in x and y could be done by using the hybrid ASM method proposed in [8]. Additionally, probe bandwidth sets an upper limit on the number of harmonics which can be recorded and renders the clinical use of the higher frequency harmonics impractical. The SVEA is however not limited to computing the harmonics of one fundamental frequency, it can have other uses: for instance, a simulation using a pulse with two frequencies has a predicted field with a spectrum with the sum and difference frequencies and their harmonics as well as the harmonics of the two fundamental frequencies. Finally, the SVEA is faster than the KZK and the INCS, and computation times are on the order of minutes. Consequently, it is possible to perform parameter sweeps in an acceptable time. Since its implementation has a similar architecture as the algorithm proposed in [4], which benefited from a 10-fold speed increase when ported on GPU [15], further developments are planned to use the NVIDIA CUDA toolkit to increase the speed, and to integrate it in the CREANUIS software [16] to perform image reconstruction.

ACKNOWLEDGMENT

This work was funded by the ANR-11 TecSan-008-01 BBMUT and was performed within the framework of the CeLyA (ANR-10-LABX-0060) of Université de Lyon, within the program Investissements d'Avenir (ANR-11-IDEX-0007) operated by the French National Research Agency (ANR). The authors would like to thank Martin Verweij, Libertario Demi, and Koen van Dongen for providing the nonlinear fields obtained with the INCS simulator.

REFERENCES

[1] M. M. Voormolen, *3D Harmonic Echocardiography:*. PhD thesis, Dept. of Biomedical Engineering, Erasmus MC, Rotterdam, The Netherlands, 2007.

[2] R. J. Zemp, J. Tavakkoli, and R. S. C. Cobbold, "Modeling of nonlinear ultrasound propagation in tissue from array transducers," *The Journal of the Acoustical Society of America*, vol. 113, no. 1, pp. 139–152, 2003.

[3] P. T. Christopher and K. J. Parker, "New approaches to nonlinear diffractive field propagation," *Journal of the Acoustical Society of America*, vol. 90, no. 1, pp. 488–499, 1991.

[4] F. Varray, A. Ramalli, C. Cachard, P. Tortoli, and O. Basset, "Fundamental and second-harmonic ultrasound field computation of inhomogeneous nonlinear medium with a generalized angular spectrum method," *IEEE Transactions on Ultrasonics, Ferroelectrics, and Frequency Control*, vol. 58, pp. 1366–1376, July 2011.

[5] Y.-R. Shen, *The principles of nonlinear optics*. Wiley classics library, Hoboken (N.J.): J. Wiley & sons, 2003.

[6] P. W. Milonni, *Laser physics*, pp. 339–340. Hoboken (N.J.): Wiley, 2010.

[7] M. Z. Kiss, T. Varghese, and M. Kliewer, "Ex vivo ultrasound attenuation coefficient for human cervical and uterine tissue from 5 to 10MHz," *Ultrasonics*, vol. 51, pp. 467–471, May 2011.

[8] U. Vyas and D. Christensen, "Ultrasound beam simulations in inhomogeneous tissue geometries using the hybrid angular spectrum method," *IEEE Transactions on Ultrasonics, Ferroelectrics, and Frequency Control*, vol. 59, pp. 1093–1100, June 2012.

[9] M. Frigo and S. Johnson, "The design and implementation of FFTW3," in *Proceedings of the IEEE*, p. 216231, 2005.

[10] J. A. Jensen, "FIELD: a program for simulating ultrasound systems," in *10th Nordicbaltic Conference on Biomedical Imaging*, vol. 4, p. 351353, 1996.

[11] J. Huijssen and M. D. Verweij, "An iterative method for the computation of nonlinear, wide-angle, pulsed acoustic fields of medical diagnostic transducers," *The Journal of the Acoustical Society of America*, vol. 127, pp. 33–44, Jan. 2010.

[12] M. D. Verweij *et al.*, "Comparison of fundamental, second harmonic, and superharmonic imaging: a simulation study," *The Journal of the Acoustical Society of America*, vol. 130, pp. 3148–3157, Nov. 2011.

[13] V. Kuznetsov, "Equation of nonlinear acoustics," *Sov. Phys. Acoustics*, vol. 16, pp. 749–768, 1970.

[14] E. Zabolotskaya and V. Kuznetsov, "Quasi-plane waves in the nonlinear acoustics of confined beams," *Sov. Phys. Acoustics*, vol. 15, pp. 35–40, 1969.

[15] F. Varray, C. Cachard, A. Ramalli, P. Tortoli, and O. Basset, "Simulation of ultrasound nonlinear propagation on GPU using a generalized angular spectrum method," *EURASIP Journal on Image and Video Processing*, vol. 2011, p. 17, Nov. 2011.

[16] F. Varray, O. Basset, P. Tortoli, and C. Cachard, "CREANUIS: a non-linear radiofrequency ultrasound image simulator," *Ultrasound in Medicine & Biology*, vol. 39, pp. 1915–1924, Oct. 2013.